



Article

# Lateral Angular Co-Extrusion: Geometrical and Mechanical Properties of Compound Profiles

Susanne Elisabeth Thürer <sup>1,\*</sup>, Julius Peddinghaus <sup>2</sup>, Norman Heimes <sup>2</sup>, Ferdi Caner Bayram <sup>3</sup> , Burak Bal <sup>3</sup>, Johanna Uhe <sup>2</sup>, Bernd-Arno Behrens <sup>2</sup>, Hans Jürgen Maier <sup>1</sup> and Christian Klose <sup>1</sup> 

<sup>1</sup> Institut für Werkstoffkunde (Institute of Materials Science), Leibniz University Hannover, 30823 Garbsen, Germany; maier@iw.uni-hannover.de (H.J.M.); klose@iw.uni-hannover.de (C.K.)

<sup>2</sup> Institut für Umformtechnik und Umformmaschinen (Institute of Forming Technology and Machines), Leibniz University Hannover, 30823 Garbsen, Germany; peddinghaus@ifum.uni-hannover.de (J.P.); heimes@ifum.uni-hannover.de (N.H.); uhe@ifum.uni-hannover.de (J.U.); behrens@ifum.uni-hannover.de (B.-A.B.)

<sup>3</sup> Department of Mechanical Engineering, Abdullah Gül University, 38080 Kayseri, Turkey; ferdicaner.bayram@agu.edu.tr (F.C.B.); burakbal@agu.edu.tr (B.B.)

\* Correspondence: thurer@iw.uni-hannover.de; Tel.: +49-511-762-18227

Received: 26 June 2020; Accepted: 26 August 2020; Published: 28 August 2020



**Abstract:** A novel co-extrusion process for the production of coaxially reinforced hollow profiles has been developed. Using this process, hybrid hollow profiles made of the aluminum alloy EN AW-6082 and the case-hardening steel 20MnCr5 (AISI 5120) were produced, which can be forged into hybrid bearing bushings by subsequent die forging. For the purpose of co-extrusion, a modular tooling concept was developed where steel tubes made of 20MnCr5 are fed laterally into the tool. This LACE (lateral angular co-extrusion) process allows for a variation of the volume fraction of the reinforcement by using steel tubes with different wall thicknesses, which enabled the production of compound profiles having reinforcement contents of either 14 vol.% or 34 vol.%. The shear strength of the bonding area of these samples was determined in push-out tests. Additionally, mechanical testing of segments of the hybrid profiles using shear compression tests was employed to provide information about the influence of different bonding mechanisms on the strength of the composite zone.

**Keywords:** tailored forming; lateral angular co-extrusion; mechanical behavior; hybrid metal components

## 1. Introduction

The realization of lightweight constructions to increase resource efficiency and reduce CO<sub>2</sub> emissions is of paramount interest to the automotive and aviation industries [1]. In particular, the use of light metals such as aluminum is attractive due to the high specific strength of the respective alloys. Merklein et al. reported that one promising approach to integrate aluminum in automotive designs is the use of hybrid components [2]. In this context, the integration of Tailored Blanks in sheet metal forming has become state of the art in the automotive industry. These allow meeting conflicting design challenges by providing sheet metal components with locally adapted properties. As well as reducing weight by combining sheets of different material grades, thicknesses, etc., Tailored Blanks can also offer improved crash performance [2].

However, the concept of hybrid semi-finished products is not yet widely used in bulk forming of metals. Innovative processing technologies are required for the production of hybrid bulk metal components made of different metals such as aluminum alloys and steel. As part of the novel concept of Tailored Forming, process chains are being developed in which the various bulk materials are

first joined before a subsequent forming process such as die forging or impact extrusion is applied. As discussed by Herbst et al., this differs significantly from conventional process chains in which the individual parts of the components are joined together after the forming step or at the end of the process chain [3].

In contrast to sheet metal forming processes used for the production of components made of Tailored Blanks, the Collaborative Research Center 1153 (CRC 1153) “Tailored Forming” aims at developing suitable processes for the production of three-dimensional solid components with locally adapted properties. The use of aluminum instead of steel in the bulk metal component can result in a reduction of mass of the component. Specifically, only the functional surface, which must be wear-resistant in the solid component, consists of material like hardened steel. A key feature in the present approach is the subsequent joint forming step. The advantage of this process combination lies in the positive influence of the subsequent forming on the local microstructure in the joining zone, and thus further the mechanical properties. This is a key aspect for materials that are difficult to form such as aluminum and steel. An exemplary process chain is shown in Figure 1 for the manufacture of a hybrid bearing bushing made of aluminum and steel that is investigated as a demonstrator part.

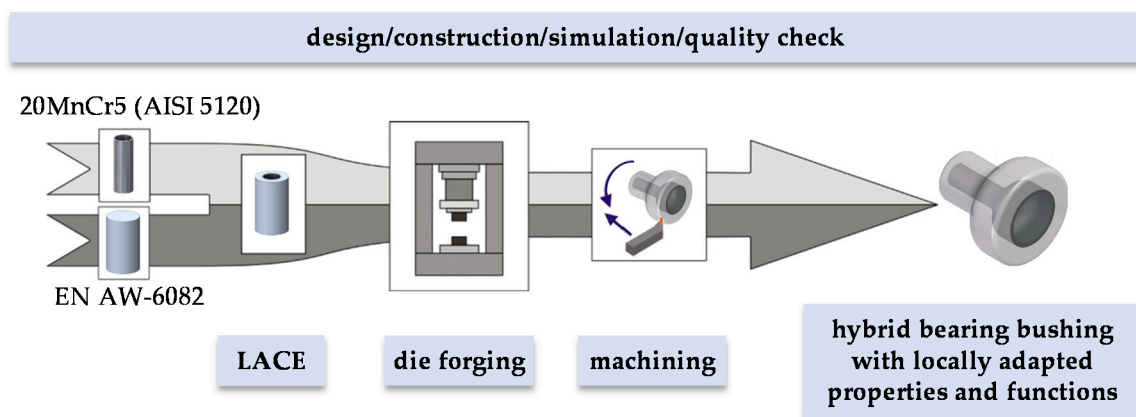


**Figure 1.** Tailored forming process chain for the production of hybrid bearing bushings.

Similar to Tailored Blanks, the production of hybrid solid semi-finished products can be realized by welding. Pressure welding is one of the processes that enables the formation of bonds in which the intermetallic phase seam is sufficiently small enough to have no negative impact on properties such as tensile strength [4]. In the context of continuous hybrid profiles, a promising approach for joining different materials is co-extrusion, which was used in the present study to manufacture the semi-finished products for the bearing bushing. Co-extrusion enables the production of composite profiles consisting of at least two materials [5]. Co-extrusion can be assigned to joining by forming according to DIN (Deutsches Institut für Normung e. V.—German Institute for Standardization) 8593-5, in which the parts to be joined are formed locally or completely. In principle, co-extrusion can be divided into two different process variants:

- Co-extrusion of modified billets: The reinforcing element is contained in the billet and passes through the entire extrusion process. This variant includes the co-extrusion of metal matrix composites in which reinforcing particles such as  $\text{Al}_2\text{O}_3$  were introduced in an aluminum billet by powder metallurgy [6] with the intention to achieve an even distribution of the reinforcing elements in the composite profile. A further variant is the local reinforcement of a billet, e.g., by inserting a round rod of a material of higher strength like titanium grade 2 into an aluminum billet and then extruding the materials simultaneously [7].
- Co-extrusion of conventional billets: In this case, the reinforcing element is introduced into the forming zone from outside the tool but is not plastically formed itself [8]. This process variant was investigated especially for the reinforcement of extruded profiles with steel or copper wires.

By employing modified chamber tools [9], the wires were introduced into the forming zone via the support arms of the mandrel. Hence, the wire reinforcement was present in the longitudinal weld seams of the profiles only [10].

With the LACE process (Lateral Angular Co-Extrusion) developed by Grittner et al., reinforcing elements such as titanium sheets and flat profiles that are already relatively rigid can be fed laterally, and thus continuously into the extrusion process [11]. A laboratory-scale LACE process has already been developed within the CRC 1153, which provided a round rod made of 20MnCr5 steel with an aluminum cladding made of EN AW-6082. However, due to the design of the tool the resulting geometry of the compound profile showed significant deviations from the desired coaxial arrangement [12]. For subsequent die forging, the steel reinforcement must be embedded coaxially within the aluminum matrix. In the present study, this issue was addressed by a novel extrusion tool design, which also featured an industry relevant scale. The mechanical properties of the bonding zones of the compound profiles produced with the new tool were characterized in push-out tests. In addition, the influence of the bonding mechanisms, e.g., material closure or form-closure, on the composite strength were determined by shear compression tests on sample segments.

## 2. Materials and Methods

### 2.1. LACE Process

A schematic section through the developed modular tool is shown in Figure 2a. Since the LACE process involves the feeding of a rigid reinforcing element instead of a wire, a mandrel part was designed, which is supported by three support arms in the tool housing. In this concept, the aluminum alloy is divided into two metal streams by the portholes in the middle of the symmetrically designed entry. Both metal strands are then directed into pockets milled into each half of the tool cavity. This is intended to change the material flow in such a way that the aluminum alloy evenly envelops the reinforcing element and displacement and/or distortion of the compound profile is avoided. The aluminum alloy then flows around the mandrel part inside the tool. The reinforcing element, in this case a steel tube, is inserted into the tool orthogonally to the movement direction of the extrusion punch and guided through the clamping cover and the mandrel part. This also ensures a coaxial position of the tube in the compound profile.

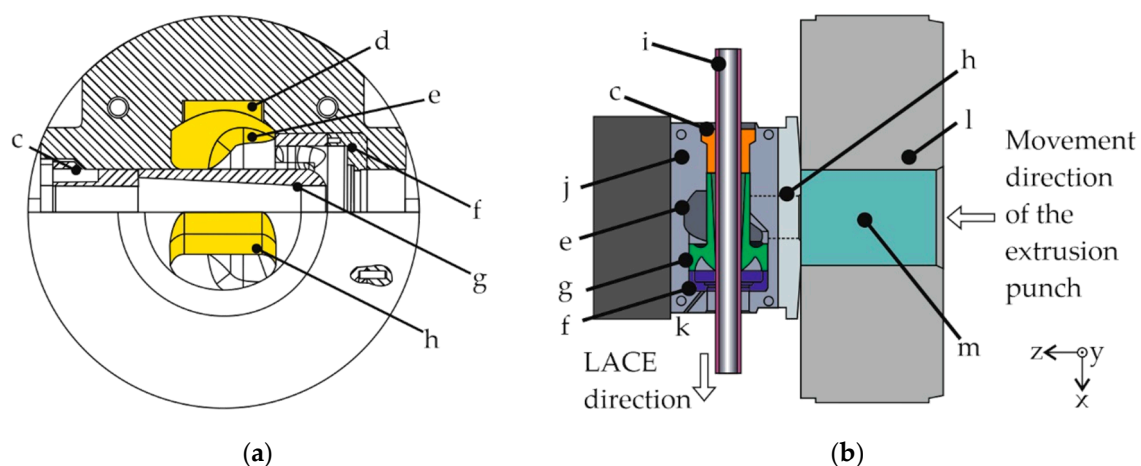


**Figure 2.** (a) Schematic illustration with sectional plane lengthwise through the tool with c: clamping cover, d: pocket, e: deflection, f: die, g: mandrel part with three support arms, h: inlet (the geometry of the inlet and deflection are highlighted); (b) schematic illustration of the concept for the 10 MN extrusion press in longitudinal section with i: reinforcing element, j: die housing, k: thermocouple bore, l: container, m: aluminum billet.

The process is shown in Figure 2b as a schematic sectional view including the reinforcing element in the tool and the billet inside the container. The LACE direction is orthogonal to the direction of the movement of the ram.

The LACE experiments were performed on a 10 MN extrusion press (SMS Meer GmbH, Düsseldorf, Germany). A non-heated tool holder specially modified for this project was used, which allowed the reinforcing element to be fed laterally. Aluminum EN AW-6082 billets as well as tubes consisting of the case-hardening steel 20MnCr5 were used as joining partners. To keep the process chain as short as possible and to avoid additional drilling of the hybrid semi-finished products, reinforcing elements with the desired inner diameter were used. Furthermore, the reinforcement content was varied by using steel tubes with different wall thickness. With an inner diameter of the container of 146 mm, an opening diameter of 62.7 mm for the die and 38 mm or 44.5 mm for the outer diameter of the steel tubes, the extrusion ratio equaled 9:1 and 11:1, respectively. This corresponds to a reinforcement content of 14 vol.% for the extrusion ratio of 9:1 and 34 vol.% for the extrusion ratio of 11:1. Since the objective was to achieve a metallurgical bond between the joining partners, the reinforcing element was ground with 40 grit paper and cleaned with ethanol prior to the extrusion process. Previous numerical studies have shown that a bond by material closure can be achieved by employing relatively high temperatures together with long contact times of the joining partners [13]. This translates to high process temperatures and low extrusion speed. Thus, the billets were preheated to 530 °C for 4.5 h, whereas the steel tube had room temperature at the beginning of each experiment. The die was preheated to 490 °C and the container had a temperature of 440 °C. A ram speed of 1.5 mm/s was used at the beginning of the experiment during the upsetting of the billet in the container and the filling of the tool, and it was reduced stepwise until the ram speed reached 0.3 mm/s. In this way, the cooling of the aluminum billet during filling of the tool was kept to a minimum.

## 2.2. Metallographic Characterization

Cross-sections were extracted from the front and the back ends of the compound profiles to determine deviations of the positions of the reinforcing elements relative to their ideal center positions, as well as to characterize the microstructures of the extruded matrix material. The front end of the actual compound profile was defined as the location where all longitudinal weld seams appeared to be macroscopically closed. The position of the back end was dependent on the particular LACE experiment. If the extrusion was stopped before the entire reinforcing element was jacketed with aluminum, the area closest to the tool was examined in cross-section. For the macro- and microstructural examination of the compound profiles, the samples were prepared metallographically and treated with an etching solution consisting of HF and H<sub>2</sub>SO<sub>4</sub> to contrast the secondary precipitates of the aluminum alloy.

## 2.3. Push-Out Test and Shear Compression Test

The mechanical properties of the bonding area of the compound profiles were measured with push-out tests and shear compression tests. For this purpose, samples were taken over the entire length of the composite profile. Due to the different coefficients of thermal expansion of aluminum and steel, the coaxially reinforced semi-finished products are assumed to have a force closure connection resulting from shrinking of the matrix material onto the reinforcing element [14]. Shear compression tests of sample segments served to determine whether the effective bond mechanism is mainly material closure or force and/or form closure. For the tests, samples were taken in an alternating order from one compound profile per extrusion ratio (Figure 3). The compound profile was divided into slices, each of which had a plane-parallel height of 10 mm after machining on both sides. The first sample was taken 25 mm behind the position, where all four longitudinal weld seams were macroscopically closed. The longitudinal weld seam that was used as the starting point of the sampling was the one closed last during extrusion and is referred to in the schematic illustration in Figure 3 as the relevant longitudinal weld seam.

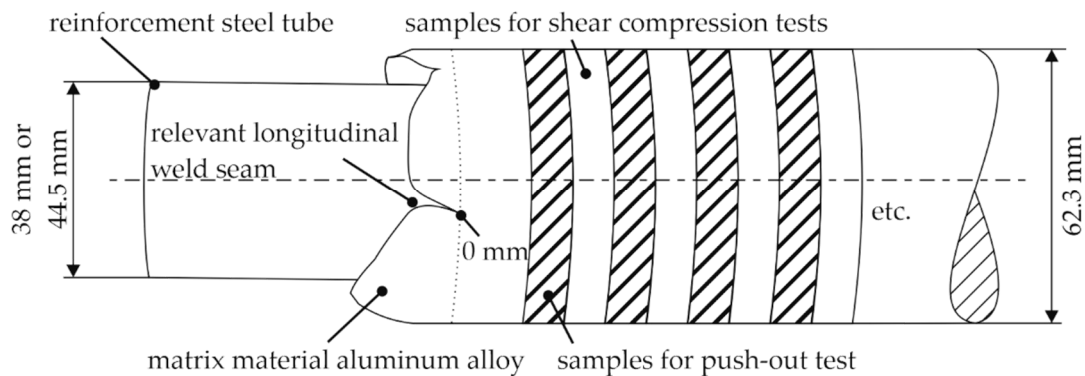


**Figure 3.** Schematic illustration of a compound profile with alternating sampling for push-out tests and shear compression tests with planned geometry of the compound profile.

Starting at this location, samples were taken from the profile with a thickness of 15 mm each, taking into account the saw cut and the allowance for facing. These samples were used as full samples for the push-out tests or divided into several segments and then used for the shear compression tests. The measured shear strength of the sample segments was then compared with the de-bonding shear strengths from the push-out tests of the adjacent samples in order to be able to determine the contribution of the material bond over the compound profile length.

The push-out tests were carried out using a universal testing machine with a maximum force of 250 kN (type Z250, Zwick, Ulm, Germany) and the test setup is shown schematically in Figure 4. Centering of the sample was realized by a step in the punch. The compound specimens were positioned on a steel ring so that the contact surface with the aluminum alloy was as large as possible. By lowering the punch of the testing machine vertically, the reinforcing element was pressed out and the force-displacement curve was recorded.

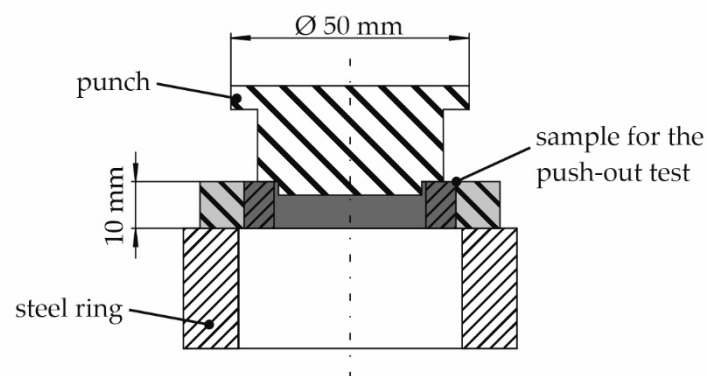


**Figure 4.** Schematic illustration of the experimental setup of the push-out tests using a sample taken from a hollow compound profile.

The specimen discs for the shear compression test, which had a plane-parallel height of 10 mm, were separated by wire cutting into the segments with an angle of about  $65^\circ$  as shown in Figure 5a. This procedure resulted in two sample segments that did not contain a longitudinal weld seam and a sample that contained two longitudinal weld seams. The latter was taken so that the longitudinal weld seams no. 1 and no. 2 (cf. Figure 5a) were at the edges of the sample segment, and thus did not affect the test results significantly. In order to determine the actual test area, the bonding lengths of all sample segments were measured by using a laser microscope (type VK 9700, Keyence, Neu-Isenburg, Germany). From these data, the actual bonding areas were calculated.

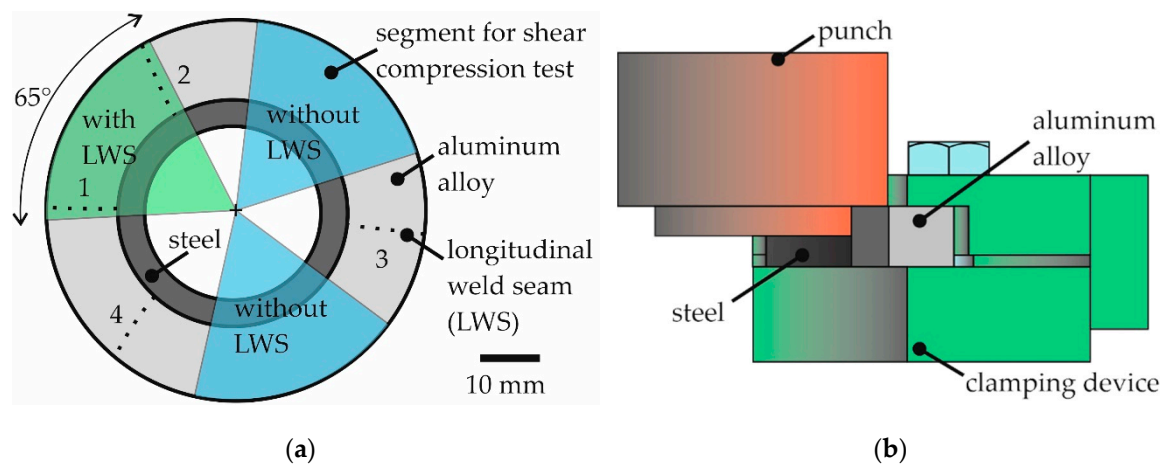


**Figure 5.** Schematic illustration of (a) sample segment extraction from the cross-section of a compound profile with one segment having two longitudinal weld seams (LWS, highlighted by dotted lines) at the edges and two segments each without weld seams, (b) test setup used for the shear compression test.

For the characterization of the mechanical properties, the specimens were clamped in the test setup shown in Figure 5b and the steel portion of the specimens was pressed out with a universal testing machine (type Z250, ZWICK, Ulm). As with the push-out tests on the entire specimen cross-sections, a test speed of  $2 \text{ mm min}^{-1}$  was used. A drop in force of 80% was used as the break-off criterion for the push-out tests of the sample segments.

### 3. Results

#### 3.1. LACE Process

During the LACE experiments, the relevant process parameters such as ram force and ram speed were recorded. Figure 6 shows an exemplary diagram of the ram force and the ram speed vs. process time for a typical LACE experiment with an extrusion ratio of 11:1. At the onset of the test, a ram speed of  $1.5 \text{ mm s}^{-1}$  was used. This fast ram speed was selected for initial filling of the tool in order to counteract cooling of the tool, whereas the actual extrusion process was performed at lower ram speed. In Figure 6, a rapid increase in ram force to a force plateau of 2.6 MN is seen. The speed of the ram was reduced to a value of  $0.5 \text{ mm s}^{-1}$  after this plateau. The ram force increased further as the filling process progressed. After reaching 5 MN, the ram speed was reduced to the desired value of  $0.3 \text{ mm s}^{-1}$  for the LACE extrusion test, which resulted in a slight drop in force. The ram force then increased continuously up to the maximum value of  $\approx 8 \text{ MN}$  before termination of the LACE process.

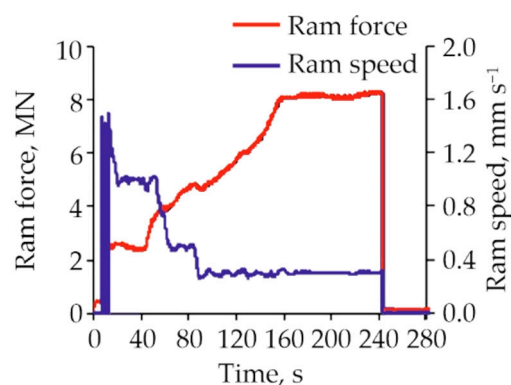


**Figure 6.** Evolution of ram force during the course of a LACE process with an extrusion ratio of 11:1 and adjustments of ram speed.

### 3.2. Metallographic Characterization

In Figure 7, representative cross-sections extracted from the front and the back ends of a compound profile are shown. Here, a steel tube with an outer diameter of  $\varnothing_a = 38$  mm was used, which resulted in an extrusion ratio of 9:1, and thus a volume fraction of the reinforcement of 14 vol.%. The outer aluminum matrix of the compound profile had a slightly elliptical cross-section at the start of the compound profile. There was a slight material overlap on the side facing the recipient (recipient side), which is interspersed with oxide lines (Figure 7a, left-hand area). The overlap on aluminum extended over a circumference of 55 mm for a total circumference of the cross-section of 202 mm. This overlap resulted from incidental clamping of the steel tube, which in turn resulted in temporarily faulty material flow. This illustrates that is of paramount importance to accurately control the local material flow in the die. For the determination of the lengths of the main and secondary axes of the aluminum jacket, this section was not taken into account. Thus, the main axis had a length  $l_y$  of 63.3 mm at the start of the profile and the secondary axis a length  $l_z$  of 63.6 mm. The outer contour was thus 1.5% larger in the y-direction and 2.0% larger in the z-direction than the theoretical diameter of the aluminum jacket. No bond was formed between the matrix material and the reinforcing element on the recipient side; instead, there was a 0.5 mm wide gap. The longitudinal weld seam on the side facing away from the recipient (rear side) also showed a gap in the bonding area between the aluminum alloy and the steel tube. By contrast, the cross-section taken from the end of the compound profile showed an almost ideal circular contour without any material overlap. The main axis had a length of 63.2 mm (deviation +1.4%) and the length of the secondary axis was 61.9 mm (deviation 0.7%).

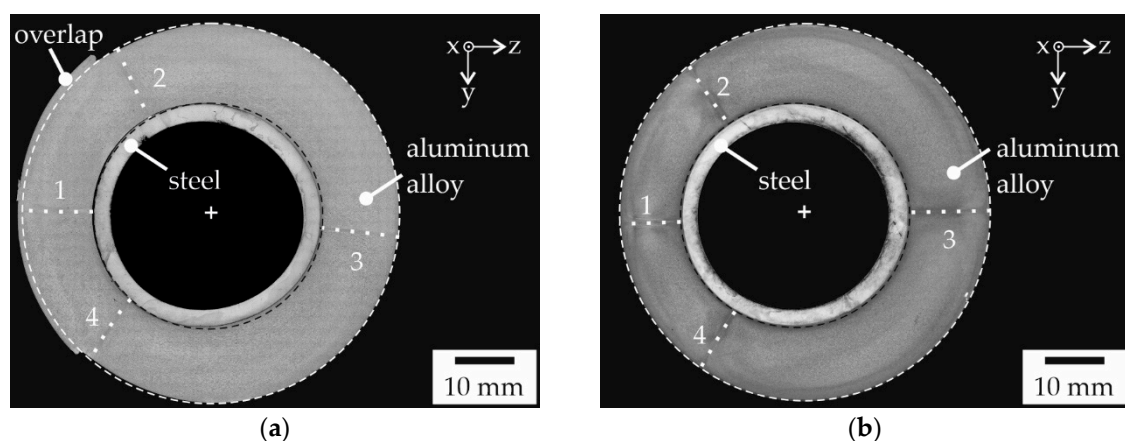


**Figure 7.** Cross-section of a sample taken from (a) the start of the compound profile, i.e., after a macroscopically closed longitudinal weld seam had formed and (b) the end of the compound profile, which was produced with an extrusion ratio of 9:1; etching: HF/H<sub>2</sub>SO<sub>4</sub> mixture; the position of the longitudinal weld seams is highlighted by dotted lines; the interpolated outer contour of the steel tube is highlighted with black dashed lines; the (in case of (a) interpolated) outer contour of the aluminum is highlighted with white dashed lines.

In the compound profile shown here, the reinforcing element was not truly embedded coaxially in the matrix. The aluminum metal stream inside the die flowed to the side facing away from the recipient preferentially. This is evident in the greater wall thickness of the matrix material on the right-hand side of the cross-sections shown in Figure 7. In the initial area of the compound profile, this led to a slight deformation of the reinforcing element, which can also be observed in Figure 7a. The reinforcing elements used in these LACE experiments were deep-hole drilled tubes with an uneven wall thickness over the tube circumference. In the compound profile shown here, the wall thickness deviated from the intended 3 mm by up to 0.5 mm, i.e., the wall thickness was between 2.7 mm and 3.5 mm. For the shown cross-section from the start of the compound profile with elliptical reinforcing element, the outer contour of the steel tube was interpolated using the theoretical outer diameter  $\varnothing_a$  of 38 mm. The offset

of the steel tube at the start of the profile was thus 0.4 mm or 0.6% in the y-direction and 0.8 mm or 1.2% in the negative z-direction. The cross-section from the end piece of the compound profile showed no geometrical deviation of the reinforcing element caused by the LACE process, despite variations in the wall thickness. The offset in the y-direction was 0.4 mm or 0.6% at the start of the profile. In the negative z-direction, the steel tube was shifted by 1.7 mm or 2.7%.

Metallographic etching was used to contrast the secondary precipitates and make the longitudinal weld seams visible. The two longitudinal weld seams that are running horizontally in the metallographic image were caused by the material flowing into the portholes of the tool entry and subsequent welding after flowing around the mandrel part or reinforcing element. Two additional longitudinal weld seams are expected on the side facing the recipient, each of which should be located at an angle of  $120^\circ$  to each other and to the longitudinal weld seam on the rear side. As seen in Figure 7, the weld seams appear close to the expected positions.

The material combination EN AW-6082 and 20MnCr5 was also extruded to a compound profile with an outer diameter of 44.5 mm for the steel tube, and thus an extrusion ratio of 11:1. The cross-sections taken from the start and end of the compound profile are shown in Figure 8a,b. Both cross-sections had almost the desired circular cross-section and did not show any deviations in the wall thickness of the steel tube, which could be attributed to deep hole drilling. The outer contour of the aluminum jacket had a length of 63.4 mm of the main axis at both the start and end of the profile (which had a length of 215 mm), which is 1.6% greater than the expected outer diameter. For the secondary axis, a length of 62.1 mm (−0.4%) could be determined at the start and 62.0 mm (0.5%) at the end of the compound profile. Residual oxides could still be detected inside the matrix material at the front end, but no longer at the back end of the compound profile. In addition, there was no complete bond between the aluminum alloy and the steel tube in the initial area, which became apparent in form of a gap with a width of  $15\ \mu\text{m}$  (detail in Figure 8c). At the end of the compound profile, this gap was no longer so pronounced (detail in Figure 8d).

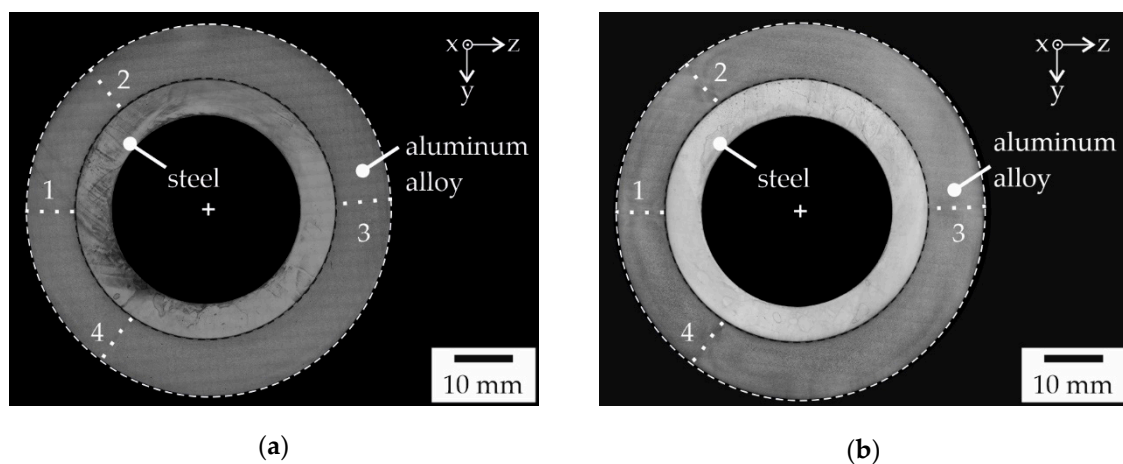
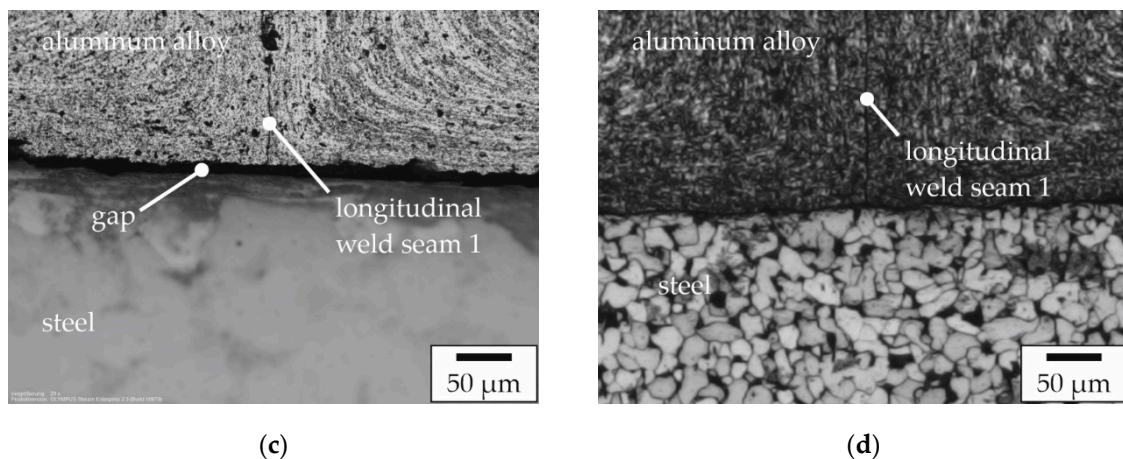


Figure 8. Cont.





**Figure 8.** Cross-sections of (a) start and (b) end of a compound profile made of EN AW 6082 and 20MnCr5 with an extrusion ratio of 11:1; the position of the longitudinal weld seams is highlighted by dotted lines; the outer contour of the steel is highlighted with black dashed lines; the outer contour of the aluminum is highlighted with white dashed lines; with (c) detailed image of the bonding area with a gap between the joining partners from the front end of the compound profile; with (d) detailed image of the bonding area from the back end of the compound profile; etching: (a–c) HF/H<sub>2</sub>SO<sub>4</sub> mixture, (d) HNO<sub>3</sub>/Ethanol mixture.

The position of the reinforcing element remained unchanged over the entire profile length and showed an offset of 0.4 mm or 0.6% in the negative *y*-direction and an offset of 0.6 mm or 0.9% in the negative *z*-direction. The position of the longitudinal weld seams did not yet correspond perfectly to the expected position at the start of the compound profile. On the one hand, the longitudinal weld seam on the recipient side was not in a perfectly horizontal position but offset in the negative *y*-direction. On the other hand, the two longitudinal weld seams, which were formed by the support arms of the mandrel part on the side facing the recipient, had a smaller angle to each other than expected. At the end of the compound profile, the longitudinal weld seams, which are formed horizontally due to the splitting of the matrix material at the portholes and subsequently by passing by one of the support arms of the mandrel part, were on the expected horizontal plane. The angle between the two longitudinal weld seams no. 2 and 4 remained unchanged.

### 3.3. Mechanical Properties

The strength of the bonding area was determined for the compound profiles with different reinforcement content using push-out tests. Figure 9 shows an exemplary force-path graph from a push-out test on a representative sample that was produced with an extrusion ratio of 11:1. At the beginning the measured force *F* increases almost linearly until the curve flattens out slightly towards the end and finally reaches its maximum *F*<sub>max</sub>. After the maximum, the force decreases rapidly and runs out in a plateau. Based on these data, the shear strength was calculated as [15]

$$\tau_{\max} = \frac{F_{\max}}{\pi d h} \quad (1)$$

where *d* is the diameter of the reinforcement and *h* the height of the sample.

Figure 10 shows the de-bonding shear strength calculated by using measured data from all the push-out tests executed over the profile length of both compound profiles. The de-bonding shear strength of the profile with the lower reinforcement content of 14 vol.% was determined over a profile length of 250 mm and varied between 29 MPa and 55 MPa with an average shear strength of 42 MPa ± 7 MPa. In the case of the profile having a reinforcement content of 34 vol.%, the shear strength determined in the push-out test varied between 45 MPa and 63 MPa over the entire profile length of 445 mm with an average shear strength of 54 MPa ± 5 MPa.

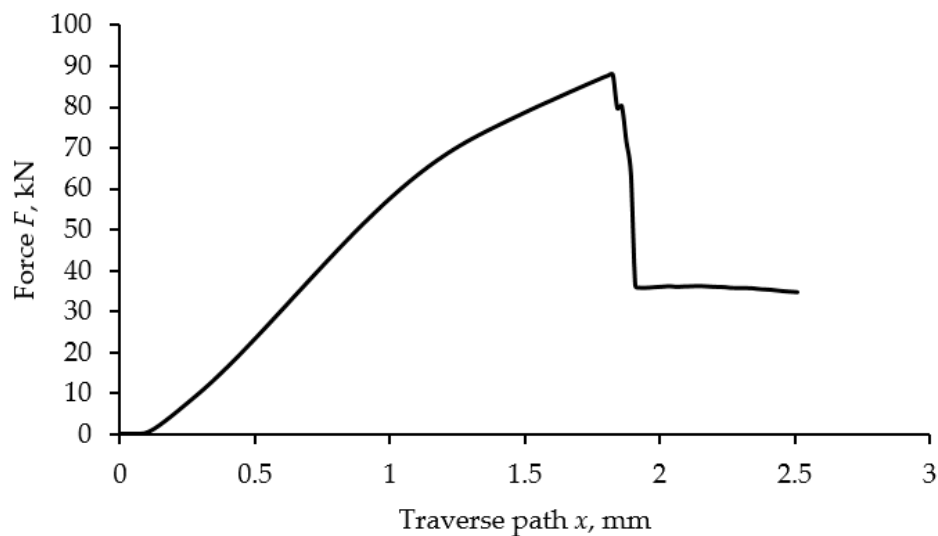


**Figure 9.** Force-displacement diagram of a push-out tests on a sample sectioned from the front end of a compound profile produced with an extrusion ratio of 11:1.

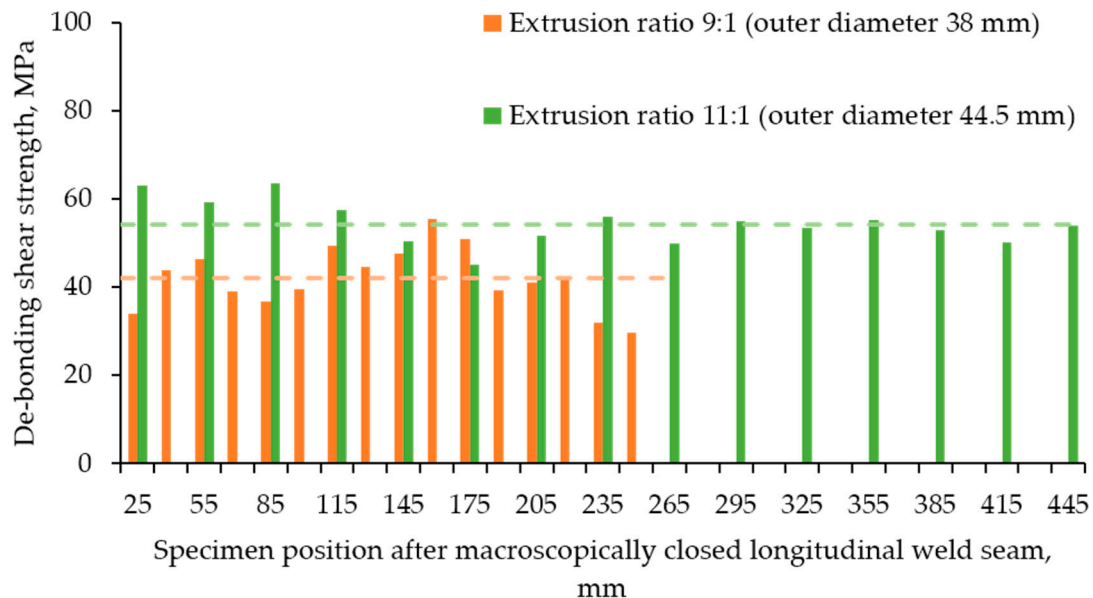


**Figure 10.** De-bonding shear strength for compound profiles produced via LACE with an extrusion ratio of 9:1 or 11:1, respectively. The respective mean values are indicated by dashed lines, which were determined over the entire length of the profile with macroscopically intact longitudinal weld seams.

For the shear compression test, two segments without longitudinal weld seams and one segment containing two longitudinal weld seams were available for each specimen cross-section. The segments without longitudinal weld seams showed a similar shear strength curve progression as the de-bonding shear strength curves determined by the push-out tests, as it can be seen in Figure 11. The values determined in the shear compression test fluctuated between 47 MPa and 69 MPa. The tested segments, which had two longitudinal weld seams, showed similar behavior over the profile length. However, there were two outliers at 100 mm and 220 mm, which, at 92 MPa and 83 MPa, respectively, had the highest strength values for the compound profiles made of the material combination EN AW-6082 and 20MnCr5. In general, the shear strength of the segment with longitudinal weld seams was below that of the segments without longitudinal weld seams from 250 mm onwards. However, the average shear strength determined in the shear compression test was 56 MPa  $\pm$  6 MPa for the segments without longitudinal weld seams and 58 MPa  $\pm$  15 MPa for the segments with longitudinal weld seams.

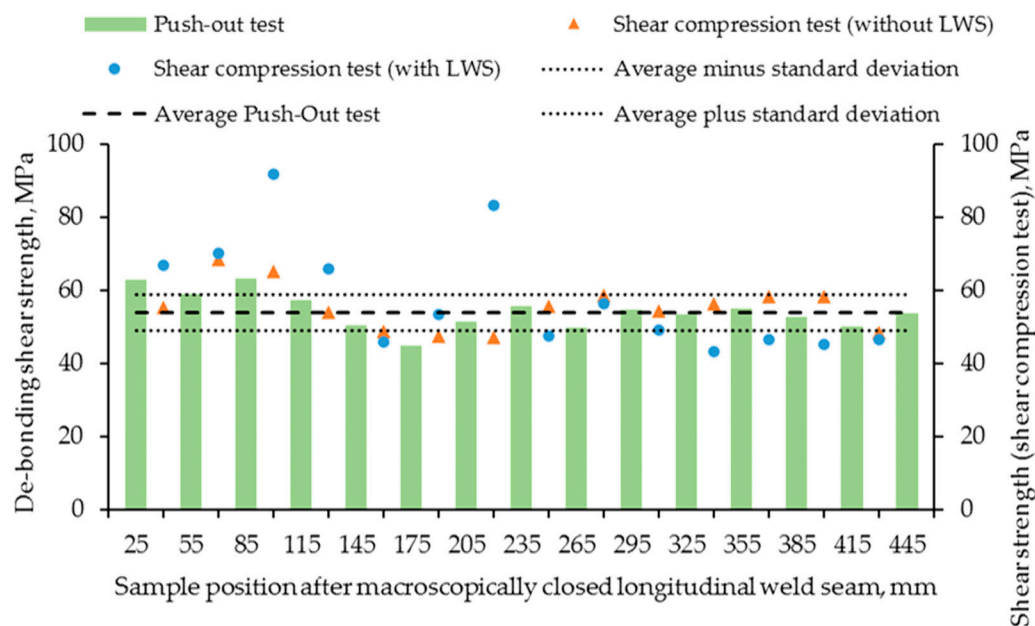


**Figure 11.** Determined shear strength of the compound profile with a reinforcement content of 34 vol.% starting 25 mm after macroscopically closed longitudinal weld seam with de-bonding shear strength averaged over the entire compound profile length (dashed line); dotted lines represent one standard deviation both for sample segments with and without longitudinal weld seams.

Figure 12 shows one of the two outliers in the shear compression test with longitudinal weld seams, extracted 100 mm behind the location where the longitudinal weld seam was considered to be macroscopically intact. The arrows and dotted lines mark the position of the longitudinal weld seams no. 1 and 2. At the position of the longitudinal weld seam no. 1, which is on the left-hand side in Figure 12, however, a gap between the joining partners can be seen. At the location of the longitudinal weld seam no. 2, which is on the right-hand side in Figure 12, it can be seen that the aluminum still adheres to the reinforcing element after the test. This demonstrates that the separation of the materials did not take place in the bonding zone.

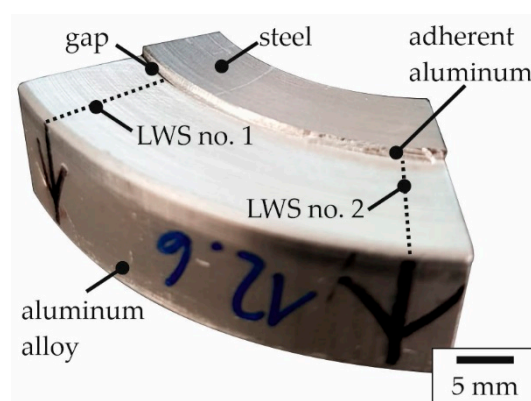


**Figure 12.** Sample after the shear compression test with adhering aluminum at the level of a longitudinal weld seam (LWS; position marked with arrows and highlighted with dotted lines).

#### 4. Discussion

In order to comply with the requirements of the intended subsequent die forging process, specifications for the compound profiles with regard to the internal geometry of the reinforcing element as well as the position of the joining partners in relation to each other were defined prior to toolset and

process development. Thus, the co-extruded semi-finished products were required to have an internal diameter  $\varnothing_i$  of 32 mm as well as an aluminum cladding with a uniform wall thickness so that the hybrid semi-finished products can be heated by means of an internal inductor prior to die-forging [16]. Furthermore, a maximum deviation in the coaxial arrangement of the joining partners of 0.2 mm (0.3%) was aimed for with a height of the semi-finished product of 85 mm. This was not fully achieved, as in some cases there was an offset of up to 0.6 mm (0.9%). By turning the semi-finished product and correspondingly increasing the length, the mold filling could still be realized in the subsequent die forging process.

In the present study, coaxially reinforced hollow profiles were produced, with a reinforcement content of 14 vol.% and 34 vol.%. With the extrusion ratio of 9:1, it was possible to envelope a steel tube having a wall thickness of 3 mm in an outer aluminum cladding without the reinforcing element collapsing due to the pressure acting on the tube during the LACE process. At the front end of the compound profile, a slight deviation of the steel tube from the desired circular geometry was detected. This deformation was no longer present at the end of the profile. A similar problem did not occur with the higher reinforcement content due to the higher wall thickness of the steel tube. Compared with previous works [12], in which a steel rod was fed into the process, a significantly improved coaxial positioning of the reinforcing element was achieved using the new guiding mandrel part and the resulting, more uniform material flow inside the novel tool. It should be noted that in the original LACE process with a titanium sheet used as external reinforcement there is no offset, since the compound profile was manufactured asymmetrically for process-related reasons [11]. However, in the case of co-extrusion processes that use wire reinforcements, deviations from the expected position of the reinforcing elements could also be detected [17]. The slight deviations observed in the present study can be explained in terms of the position on the feeding of the reinforcement via a mandrel part. For the application in the process chain of the CRC 1153, the offset could be compensated by further adjustment of the tool or using turned semi-finished products.

The metallographic characterization has revealed that the gaps between the matrix material and the reinforcing element were present on the recipient side in the initial parts of the compound profile. However, these gaps between aluminum and steel were no longer detected in any tests at the end of the compound profile. Thus, these gaps will not be relevant in a Tailored Forming process chain for the production of hybrid bearing bushings once steady-state conditions are attained.

At  $42 \text{ MPa} \pm 7 \text{ MPa}$ , the average shear strength of the profile produced with the lower extrusion ratio was slightly lower than that of the profile with the higher extrusion ratio, i.e., the one with the higher volume fraction of reinforcement. For the latter, an average shear strength of  $48 \text{ MPa} \pm 9 \text{ MPa}$  was measured. These values are below the composite strengths that were determined for a LACE process conducted on a laboratory scale [18]. However, since the compound profiles manufactured in these earlier experiments showed a clear warping, their higher bond strengths are attributed to the more pronounced force and form closure.

Compared with the shear strengths achieved in push-out tests on compound forged bearing bushings investigated by Behrens et al. [16], the shear strength achieved with semi-finished products manufactured by LACE was about 20 MPa lower. The bond formation in the compound forging was thus somewhat better, which can be substantiated by the joint forming, and thus by the more extensive formation of new surfaces in the process [14]. In the LACE process, on the other hand, only the aluminum is formed and the relative movement of the materials to each other [11] forms the joint between the partners. The strength of the joining zones is nevertheless promising to withstand the subsequent die forging process.

Due to the coaxial arrangement of the joining partners inside the LACE tool, it can be assumed that the higher thermal expansion coefficient of aluminum causes shrinking of the outer EN AW-6082 cladding onto the steel tube, which results in a form closure as well as a force closure [14]. However, a firm connection that will withstand subsequent bulk forming processes such as forging, requires material closure, as this connects the joining partners by means of physical or chemical bonds,

so that they function as one body [19]. Whether the desired material closure is present in the LACE samples, was therefore tested using shear compression tests on segments taken from the sample cross-sections. The existing form and force closures were released by cutting out 65° segments from the sample cross-section.

With respect to the subsequent forging operation, the interface properties are of paramount importance. Ideally, a firm metallurgical bond should be formed. Depending on the process conditions, brittle intermetallic phase can growth at the interface between the joining partners. Herbst et al. reported that intermetallic phase seams narrower than 1 µm have no negative effect on the strength of the composite [3]. In the present study, no intermetallic phase seams were detected metallographically. In addition, due to the coaxial arrangement of the joining partners inside the LACE tool, it can be assumed that the higher thermal expansion coefficient of aluminum causes shrinking of the outer EN AW-6082 cladding onto the steel tube. This will result in a form closure as well as a force closure [14]. However, subsequent bulk-forming processes, such as forging, require material closure, i.e., a firm connection by means of physical or chemical bonds, so that they function as one body [19]. Whether the desired material closure was realized in the LACE samples, was therefore tested using shear compression tests on segments taken from the sample cross-sections. The existing form and force closures were released by cutting out 65° segments from the sample cross-section.

The LACE profile with a steel tube made of 20MnCr5 had a shear strength of 54 MPa ± 5 MPa over the entire profile length, which was determined in the push-out test. The segments without longitudinal weld seams showed almost identical shear strengths with values of 56 MPa ± 6 MPa and the samples with two longitudinal weld seams showed no change over the averaged total profile length, resulting in a value of 58 MPa ± 15 MPa. The strength of the specimen with longitudinal weld seams was both above and below the strength of the segments without longitudinal weld seams. Only the increased deviation in the values shows a slight influence of the longitudinal weld seams on the shear strength. It can therefore be assumed that the proportion of form-fit or frictional connection in the samples manufactured using LACE is low. The shear compression test of the specimens with longitudinal weld seams has shown that the longitudinal weld seams can have a positive influence on the shear strength. The aluminum adhered clearly to the steel near a longitudinal weld seam, which was formed by splitting by a support arm of the mandrel part. The splitting of the aluminum flow and re-welding in the welding chamber thus produced juvenile metal surfaces, which had a positive influence on the formation of the bonding area. According to Weidenmann et al., material closure is also assumed if the reinforcing element is covered by residues of the matrix material after a shear compression test [20], which was the case here for most of the tested samples.

## 5. Conclusions and Outlook

It could be shown that quasi-continuous hybrid hollow profiles made of EN AW-6082 and 20MnCr5 can be produced on an industrial-relevant scale by employing a lateral angular co-extrusion process together with a new tool concept. The modular design allows the extrusion ratio to be increased, e.g., from 9:1 to 11:1, and thus the reinforcement content could be varied between 14 vol.% and 34 vol.%. The placement of the steel tube inside the aluminum cladding deviated slightly from the desired ideal coaxial position. The de-bonding shear strengths determined by push-out tests were between 42 MPa and 47 MPa. The shear compression tests on sample segments showed that not only form-fit and force-fit is present between the aluminum alloy and the steel tube. The aluminum residues adhering to the steel after the shear compression tests also indicate a material-locking connection, which was observed especially in the areas next to the longitudinal weld seams. The bonding area of these samples needs be investigated more closely in the future to be able to fully exploit the potential of the LACE process.

**Author Contributions:** Conceptualization, H.J.M., C.K. and B.-A.B.; methodology, S.E.T., J.P. and F.C.B.; validation, S.E.T., N.H. and J.U.; investigation, S.E.T.; writing—original draft preparation, S.E.T.; writing—review and editing, H.J.M., J.U., B.B. and C.K.; visualization, S.E.T.; supervision, H.J.M., C.K. and B.-A.B.; project administration, H.J.M., C.K. and B.-A.B.; funding acquisition, H.J.M., C.K. and B.-A.B. All authors have read and agreed to the published version of the manuscript.

**Funding:** This study was funded by the Deutsche Forschungsgemeinschaft (DFG, German Research Foundation)—CRC 1153, subproject A1—252662854. The authors thank the DFG for financial support.

**Acknowledgments:** The results presented were obtained within the subproject A1 “Influence of local microstructure on the formability of extruded composite profiles” of the Collaborative Research Centre 1153 “Process chain to produce hybrid high performance components by Tailored Forming”.

**Conflicts of Interest:** The authors declare no conflict of interest.

## References

- Hirsch, J.; Hirsch, J. Aluminium in Innovative Light-Weight Car Design. *Mater. Trans.* **2011**, *52*, 818–824. [[CrossRef](#)]
- Merklein, M.; Johannes, M.; Lechner, M.; Kuppert, A. A review on tailored blanks—Production, applications and evaluation. *J. Mater. Process. Technol.* **2014**, *241*, 151–164. [[CrossRef](#)]
- Herbst, S.; Maier, H.J.; Nürnberger, F. Strategies for the Heat Treatment of Steel-Aluminium Hybrid Components. *HTM J. Heat Treat. Mater.* **2018**, *73*, 268–282. [[CrossRef](#)]
- Agudo, L.; Jank, N.; Wagner, J.; Weber, S.; Schmaranzer, C.; Arenholz, E.; Bruckner, J.; Hackl, H.; Pyzalla, A. Investigation of microstructure and mechanical properties of steel-aluminium joints produced by metal arc joining. *Steel Res. Int.* **2008**, *79*, 530–535. [[CrossRef](#)]
- Bauser, M.; Sauer, G.; Siegert, K. *Strangpressen*; Aluminium-Verlag: Düsseldorf, German, 2001; ISBN 3-87017-249-5.
- Foydl, A.; Haase, M.; Ben Khalifa, N.; Tekkaya, A. Co-extrusion of discontinuously, non-centric steel-reinforced aluminum. In Proceedings of the the 14th International Esaform Conference on Material Forming, Esaform 2011, Menary, Gary, 27–29 April 2011; pp. 443–448.
- Dietrich, D.; Grittner, N.; Mehner, T.; Nickel, D.; Schaper, M.; Maier, H.J.; Lampke, T. Microstructural evolution in the bonding zones of co-extruded aluminium/titanium. *J. Mater. Sci.* **2013**, *49*, 2442–2455. [[CrossRef](#)]
- Kleiner, M.; Schomäcker, M.; Schikorra, M.; Klaus, A. Herstellung verbundverstärkter Aluminiumprofile für ultraleichte Tragwerke durch Strangpressen. *Mater. Werkst.* **2004**, *35*, 431–439. [[CrossRef](#)]
- Pietzka, D.; Ben Khalifa, N.; Gerke, S.; Tekkaya, A. Composite extrusion of thin aluminum profiles with high reinforcing volume. *Key Eng. Mater.* **2013**, *554*, 801–808. [[CrossRef](#)]
- Weidenmann, K.A. *Verbundstrangpressen Mit Modifizierten Kammerwerkzeugen: Werkstofftechnik, Fertigungstechnik, Simulation*. Karlsruhe; KIT Scientific Publishing: Karlsruhe, Germany, 2012; ISBN 978-3-86644-890-2.
- Grittner, N.; Striwe, B.; Von Hehl, A.; Engelhardt, M.; Klose, C.; Nürnberger, F. Characterization of the interface of co-extruded asymmetric aluminum-titanium composite profiles. *Mater. Werkst.* **2014**, *45*, 1054–1060. [[CrossRef](#)]
- Thürer, S.E.; Uhe, J.; Golovko, O.; Bonk, C.; Bouguecha, A.; Klose, C.; Behrens, B.-A.; Maier, H.J. Co-extrusion of semi-finished aluminium-steel compounds. In Proceedings of the 20th International Esaform Conference on Material Forming: Esaform 2017, Dublin, Ireland, 26–28 April 2017; p. 140002.
- Behrens, B.-A.; Klose, C.; Thürer, S.E.; Heimes, N.; Uhe, J. Numerical modeling of the development of intermetallic layers between aluminium and steel during co-extrusion. In Proceedings of the 22nd International Esaform Conference on Material Forming: Esaform 2019, Vitoria-Gasteiz, Spain, 8–10 May 2019; p. 040029.
- Behrens, B.-A.; Kosch, K.-G. Development of the heating and forming strategy in compound forging of hybrid steel-aluminum parts. *Mater. Werkst.* **2011**, *42*, 973–978. [[CrossRef](#)]
- Weidenmann, K.; Kerscher, E.; Schulze, V.; Löhse, D. Characterization of the interfacial properties of compound-extruded lightweight profiles using the push-out-technique. *Mater. Sci. Eng. A* **2006**, *424*, 205–211. [[CrossRef](#)]

16. Behrens, B.-A.; Sokolinskaja, V.; Chugreeva, A.; Diefenbach, J.; Thüerer, S.; Bohr, D. Investigation into the bond strength of the joining zone of compound forged hybrid aluminium-steel bearing bushing. In Proceedings of the 22nd International Esaform Conference on Material Forming: Esaform 2019, Vitoria-Gasteiz, Spain, 8–10 May 2019; p. 040028.
17. Pietzka, D. *Erweiterung des Verbundstrangpressens zu Höheren Verstärkungsanteilen und Funktionalen Verbunden*; Kleiner, M., Ed.; Shaker Verlag: Düren/Maastricht, Germany, 2014.
18. Thüerer, S.E.; Uhe, J.; Golovko, O.; Bonk, C.; Bouguecha, A.; Behrens, B.-A.; Klose, C. Mechanical properties of co-extruded aluminium-steel compounds. *Key Eng. Mater.* **2017**, *742*, 512–519. [[CrossRef](#)]
19. VDI-Fachbereich Produktentwicklung und Mechatronik. *Methodische Auswahl Fester Verbindungen-Systematik, Konstruktionskataloge, Arbeitshilfen*; VDI-Gesellschaft Produkt- und Prozessgestaltung: Düsseldorf, Germany, 2004.
20. Weidenmann, K.A.; Kersch, E.; Schulze, V.; Löhe, D. Grenzflächen in verbundstrangpressprofilen auf aluminiumbasis mit verschiedenen verstärkungselementen. In *Praktische Metallographie Sonderband 37*; Göken, M., Ed.; KIT Scientific Publishing: Karlsruhe, Germany, 2005; pp. 131–136.



© 2020 by the authors. Licensee MDPI, Basel, Switzerland. This article is an open access article distributed under the terms and conditions of the Creative Commons Attribution (CC BY) license (<http://creativecommons.org/licenses/by/4.0/>).